Proceedings of the 18th Iranian Geophysical Conference, May 2018, pages 316-319

A comparison of individual and combined classification methods for processing of ASTER data

H. Jamshid Moghadam[1], M. Mohammady Oskuei[2], N. Azadi[3]

[1]*PhD student, Faculty of Mining Engineering, Sahand University of Technology, Tabriz, hj_moghadam@sut.ac.ir*
[2] *Associate Professor, Faculty of Mining Engineering, Sahand University of Technology, Tabriz, mohammady@sut.ac.ir*
[3]*PhD student, Faculty of Mining Engineering, Sahand University of Technology, Tabriz, No_azadi@sut.ac.ir*

ABSTRACT
Mineral mapping using remote sensing techniques has been developed for application in the field of deposit exploration. However, the classification methodology in the processing of satellite images is one of the most important steps that affects the accuracy of resultant maps. An integration use of several classifiers is a helpful strategy to achieve more accurate results. The study aims to classify an ASTER scene with the use of Hyperion unmixing results of Lahrud, Iran. The detected minerals by Mixture Tuned Matched Filtering (MTMF) method on Hyperion image were used as training classes. The separability score was computed between classes imported from Hyperion data analysis. In order to improve the accuracy of upcoming processes, classes with high similarity (with low separability) were combined. Therefore, 6 classes with adequate separability score were determined as final classes for classification. The classification of ASTER scene was then performed with the use of four individual and four combined classifiers. An accuracy analysis was performed to compare the functionality of each classifier and the Max rule method demonstrated the best performance among all classifiers tested in this study regarding to its highest overall accuracy.
Keywords: Remote sensing, ASTER, Classification, Combined classification, Hyperion, Overall accuracy.

INTRODUCTION
Processing of satellite optical data in detection of geological features like rock type, contacts, linear and circular structures, and alteration zones is either directly or indirectly useful in mineral deposits exploration. Classification plays an important role in information extraction from satellite data. The pixels spectrums are therefore compared to the training data set based on a criterion that expresses the "similarity". The individual classifiers are generally applied for this goal. However, the combined methods can sometimes improve the resultant accuracy (Richards and Jia 2006).
More statistical methods in the field of classification were developed by Swain (1981); and Kittler and Pairman (1985). Kittler et al (1998) made a theoretical framework for various combined classifiers and compared different combination schemes. In recent years, new techniques of combined classification methods for improving accuracy of image are presented [Lepistö et al. 2004; Li and Zong 2007; Salah et al. 2010; Bruzzone and Demir 2014; Li and Wan 2015].
This study aims to classify an ASTER scene with the use of Hyperion unmixing results in Lahroud area, NW Iran. Therefore, the separability scores among training classes were computed. Four individual and four combined classification methods was then performed. Finally, a comparison was made between the various methods.

STUDY AREA
The area under investigation is located in the northwest of Iran (47° 37′ 48.94″E and 39° 4′ 22.7″N). This area is a part of the Lahroud 1:100K geological map. It is situated in the Alborz-Azerbaijan structural zone. The lithology of the region is generally related to the cenozoic era. Three main alteration types have been detected in the Lahroud sheet including the alunite, kaolinite, and silicified zones, covering 56.3% of the study area. One of the indicators of Azerbaijan – Alborz zone is the analcime lavas and broadly covered the region (Ghandchi et al.1991; Oskuei and Babakan 2016).

DATA DESCRIPTION
ASTER datasets generally includes 14 channels in three VNIR, SWIR, and TIR wavelength ranges. Ground resolutions of those three groups are different (VNIR: 15m, SWIR: 30m, TIR: 90m). Each ASTER scene covers an area of 60 × 60 km (Hashemi Tangestani and Azizi 2011).
The MTMF, a spectral matching method, was used to produce image maps which can show the distribution and abundance of selected minerals. MTMF results of Hyperion data analysis were employed as training data. Table 1 illustrates ten detected minerals for each distinguished endmember (Boardman 1998).

Table 1. Detected minerals for each endmember using MTMF.

Endmembers(Classes)	Minerals	Endmembers(Classes)	Minerals
1	Scapolite(silicate minerals)	6	Analcime
2	Carnalit(Poly halite)	7	Malachit
3	Analcime or natrolite	8	Kainite(Poly halite)
4	Carnalit (Poly halite)	9	Carnalit(Poly halite)
5	Analcime or natrolite	10	Scapolite + Analcime

TRAINING DATA

The Hyperion scene was registered on the ASTER image for adjusting of their pixel size and coordination. Therefore, the obvious tie points were selected as control points (Figure 1a). Correlation between the control points is significant and the selected points must be well distributed. The MTMF rule channels were then resampled on ASTER scene as ten classes. Figure 1b illustrates the reconcile image of the MTMF maps on the ASTER image (classes 1 to 10). Separability analysis was performed in order to evaluate the ability of ASTER data to spectrally discriminate among different classes. Therefore, the spectrally separable classes will provide higher classification accuracies.

Generally, the outputs separability value of two classes is between 0.0 and 2.0. Values near 2 reveals a high degree of separability, while 0 indicates the lowest separability and the class pairs with lower separability values (less than 1) should be combined into a single class (Thomas et al. 2003). The resultant scores for each pair of classes were tabulated in table 2. Only a few pairs show scores more than 1.0 which is not satisfactory. Therefore, the classification using these classes will not result in appropriate accuracy. The classification of the MTMF rule image with higher thresholds will decrease the number of pixels in each class and their spectral overlaps. The separability scores were then calculated for different thresholds. The separability for a certain number of 500, 1000, 3000, 5000 pixels in each class were investigated. Using of 500 pixels as training data resulted in the best possible separability scores as demonstrated in table 3. Thus, the classes (2, 4, 8, 9) and (3, 5) were merged due to their low separability. This means that now we can classify the ASTER dataset for 6 training classes [(1), (2-4-8-9), (3-5), (6), (7), (10)]. Table 4 illustrates the final training data for classification.

Table 2. Separability computation for maximum map classes.

Classes	2	3	4	5	6	7	8	9	10
1	0.9424	**1.4943**	0.6542	0.6752	0.8537	0.5491	0.4500	0.9393	0.6418
2		**1.1550**	0.1460	0.2534	0.2696	0.2247	0.2138	0.2320	0.1984
3			**1.1385**	0.2819	**1.1086**	**1.0613**	**1.2214**	**1.3344**	**1.0613**
4				0.1182	0.1978	0.1785	0.1256	0.1680	0.0650
5					0.4521	0.3007	0.1840	0.2631	0.2295
6						0.3356	0.3821	0.3640	0.1384
7							0.0957	0.4506	0.1551
8								0.3227	0.1686
9									0.2581

Table 3. Separability computations when a number of 500 pixels of each band MTMF is selected.

Classes	2	3	4	5	6	7	8	9	10
1	1.9271	1.9938	1.9503	1.9984	1.9814	1.2557	1.6609	1.9780	1.8964
2		1.8876	**0.1257**	1.9381	1.0242	1.8294	**0.7102**	**0.2327**	1.4749
3			1.9168	**0.3559**	1.8327	1.9541	1.8995	1.9206	1.9256
4				1.9566	1.0303	1.8671	**0.9077**	1.1800	1.4600
5					1.8819	1.9801	1.9480	1.9572	1.9602
6						1.9137	1.5991	1.9127	1.8319
7							1.4867	1.9278	1.8536
8								1.1630	1.4172
9									1.6407

Table 4. Final training classes for classification.

Endmembers(Classes)	Minerals	Endmembers(Classes)	Minerals
1	Scapolite (silicate minerals)	6	Analcime
2-4–8-9	Poly halite	7	Malachit
3-5	Analcime or natrolite	10	Scapolite + analcime

Table 5. Producer and overall accuracy (%) for each classification method.

		Classes								
		1	2-4-8-9	3-5	6	7	10	Max	Min	OA
Methods	ML	**43.00**	59.67	37.06	**16.34**	7.01	29.18	59.67	7.01	**30.45**
	SVM	27.49	**63.10**	**37.34**	6.05	5.81	14.62	63.10	5.81	23.12
	ANN	33.33	53.83	34.93	14.84	**16.15**	12.76	53.83	12.76	25.08
	SAM	25.23	26.89	30.16	21.46	4.16	**41.72**	41.72	4.16	22.15

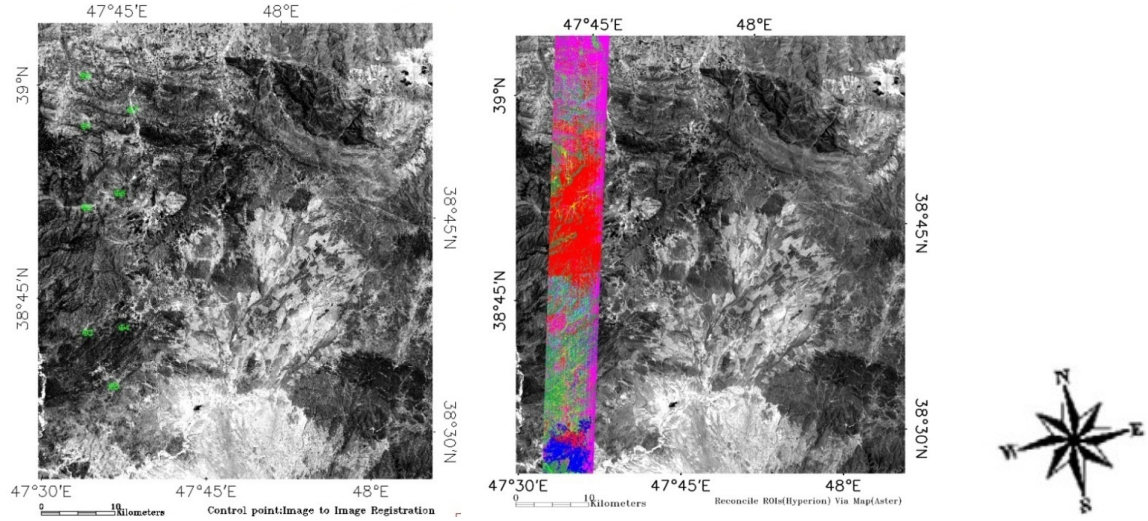

(a) (b)

Figure 1. a) location of the control points. b) reconciled image of MTMF map on the ASTER scene.

CLASSIFICATION

Generally, the classification of satellite images aims to cluster the image pixels into discrete spectral classes and the resulting classified image is essentially a thematic map of the original image. In the supervised classification methods, the analyst selects samples of the different elements as training data to identify in the image. In this method the analyst knowledge of the study area determines the quality of the training set. The pixels assigned for each class most closely resembles digitally. The difference among the types of supervised classifiers is that how they determine similarity between pixels (Schowengerdt 2012).

Four supervised classification methods: Maximum Likelihood (ML), Support Vector Machine (SVM), Artificial Neural Network (ANN) and Spectral Angle Mapper (SAM) were applied to perform the task. For each classification, the confusion matrix using classified and control pixels were constructed. The producer accuracy (PA) and overall accuracy (OA) was then computed to evaluate the performance of classification algorithms.

In table 5, the PAs of the classifiers are indicated for 6 classes. The last column in the table is the OA of each classifier. In accordance with the results obtained by the confusion matrix, the ML classifier showed a good performance among individual classification methods.

The individual classification methods for useful combination should be different in nature. In addition, the appropriate combination rule is used for results incorporation, so that covers each other's weaknesses. Four common combined classifiers (i.e; product, sum, maximum, and median rule) were run with the use of calibrated rule images in the range from 0.0 to 1.0. The resulting accuracies of these classifiers were demonstrated in table 6. According to the results, the maximum rule method has most accurate performance among the mentioned combined classifiers. Figure 2 illustrates the thematic maps with the use of ML and Maximum rule methods.

Table 6. Overall accuracy resulted (%) by four combined classification.

	Classifiers			
	Product rule	Sum rule	Maximum rule	Median rule
OA,%	29.00	29.12	**34.26**	29.08

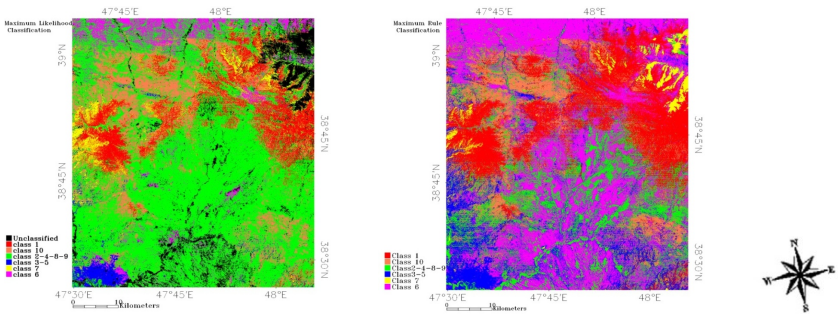

(a) (b)

Figure 2. The resultant classification map by ML (a) and Maximum rule (b) methods.

CONCLUSION

The integrated use of the ASTER and Hyperion datasets was applied for achieving better accuracy and reducing time and cost effectively. Therefore, the results of Hyperion data unmixing processes were used as training classes for the classification of the ASTER scene.

The classification was performed with the use of four individual classifiers including ML, SAM, ANN and SAM. The accuracy evaluation implied that among them the ML method yields the most accurate results. Meanwhile, the capability of combined classification was also investigated. Four common combined classifiers was performed. The Max rule method yielded the best performance among the individual and combined classifiers method regarding to its highest overall accuracy.

REFERENCES

Richards, J.A., and Jia, X. (2006). Remote sensing Digital Image Analysis an Introduction, 4th Edition, Springer, Germany, Berlin, Heidelberg.

Lepistö, L., Kunttu, I., Autio, J., and Visa, A. (2004). Combining Classifiers in Rock Image Classification – Supervised and Unsupervised Approach. In Proc. of Advanced Concepts for Intelligent Vision Systems, Brussels, Belgium.

Li, S., and Zong, C. (2007). Classifier Combining rules under Independence Assumption. MCS'07 proceeding of the 7th International Conference on Multiple classifier, Springer-verlag Berlin, Heidelberg, PP. 322-332.

Salah, M., Trinder, J., Shaker, A., Hamed, M., and Elasagheer, A. (2010). Integrating Multiple Classifiers with Fuzzy Majority voting for improved landcover classification. In: IAPRS, Vol. XXXVIII, Part 3A – Saint-Mandé, France, September 1-3.

Bruzzone, L., and Demir, B. (2014). A Review of Modern approaches to Classification of Remote sensing Data. Remote sensing and Digital image processing, Vol.18, PP. 127 – 143.

Li, G., and Wan, Y. (2015). A new combination classification of pixel and object based methods. International Journal of Remote Sensing, Vol.36, NO.23, PP. 5842 – 5868.

Ghandchi, M., Afsharian Zadeh, A., and Chaychi, Z. (1991). "1:100000 Geological Map of Lahrud", Geologocal Survey of Iran.

Oskuei, M.M., and Babakan, S. (2016). Role of Smile Correction in Mineral detection on Hyperion data. Journal of Mining & Environment(JME). Vol.7, NO.2, PP. 261 – 272.

Hashemi Tangestani, M., and Azizi, M. (2011). Evaluation of pixel and sub pixel classification of Aster data for the spetial distribution detection of clay minerals (case – study: Esteghlal mine, Abadeh). Iranian journal of Remote sensing & GIS. Vol. 2, No. 4, pp. 101-118.

Boardman, J.W.. (1998). Leveraging the high dimensionality of AVIRIS data for improved sub-pixel target unmixing and rejection of false positives: Mixture Tuned Matched Filtering. In: Proceedings of the 7th Annual JPL Airborne Geoscience Workshop, JPL Publication 97-21, P. 55. Pasadena, CA.

Thomas, V., Treitz, P., Jelinski, D., Miller, J., Lafleur, P., and McCaughey, J.H. (2003). Image Classification of a northern peatland complex using spectral and plant community data. Remote - Sensing of Environment 84, No.1, pp. 83-99.

Schowengerdt, R.A. (2012). Techniques for Image Processing and Classification in Remote Sensing. Academic Press, London.